Tussilagone Inhibits Osteoclastogenesis and Periprosthetic Osteolysis by Suppressing the NF-κb and p38 MAPK Signaling Pathways

Xuantao Hu
The Second Xiangya Hospital
Zhengxiao Ouyang (ouyangzhengxiao@csu.edu.cn)
Second Xiangya Hospital https://orcid.org/0000-0002-8997-0446
Dan Peng
The Second Xiangya Hospital
Ziqing Yin
The Second Xiangya Hospital
Xia Chen
The Second Xiangya Hospital
Guangyao Jiang
The Second Xiangya Hospital
Daishui Yang
The Second Xiangya Hospital
Ziqin Cao
The Second Xiangya Hospital
Shuai Li
The Second Xiangya Hospital
Zicheng Liu
The Second Xiangya Hospital

Research

Keywords: Tussilagone, osteoclast, NF-κB, p38, MAPK, aseptic prosthetic loosening, periprosthetic osteolysis

Posted Date: December 31st, 2019

DOI: https://doi.org/10.21203/rs.2.19812/v1

Abstract

Backgroud: Aseptic prosthetic loosening is one of main factor producing poor prognosis of limb function after joint replacement and requiring troublesome revision surgery. It is featured by wear particle–induced periprosthetic osteolysis mediated by excessive osteoclasts activated in inflammatory cell context. In our previous study, some natural compounds showing anti-osteoclast trait with high cost-efficiency and few side effects. Tussilagone (TUS), as the main functional extract from Tussilago Farfara precedently used for relieving cough, asthma and eliminating phlegm in traditional medicine, has been proved to appease several RAW264.7-mediated inflammatory diseases via suppressing osteoclast-related signaling cascades. However, whether and how TUS can improve aseptic prosthetic loosening via modulating osteoclast-mediated bone resorption still need to be answered.

Methods: We established a murine calvarial osteolysis model to detect the preventative effect of TUS on osteolysis *in vivo*. Micro-CT scanning and histomorphometric analysis were used to determine the variation of bone resorption and osteoclastogenesis in samples. The anti-osteoclast-differentiation and anti-bone-resorption bioactivities of TUS *in vitro* were investigated using bone slice resorption pit evaluation and interference caused by cytotoxicity of TUS was excluded according to CCK-8 assay. Quantitative PCR analysis was applied to prove the decreased expression of osteoclast-specific genes after TUS treatment. The inhibition effect of TUS on NF-κb and p38 MAPK signaling pathways was testified by western blotting and NF-κB-linked luciferase reporter gene assay.

Results: TUS demonstrated bone protective effect against osteolysis in murine calvarial osteolysis model with reduced osteoclasts compared to the control group. Following studies *in vitro* witnessed that TUS exert anti-osteoclastogenesis and anti-bone-resorption effects in both BMMs and RAW264.7 cells, as evidenced by the decline of osteoclast specific genes according to quantative PCR. Western blotting revealed that TUS-treated demonstrated inhibited IκBα degradation and p38 phosphorylation.

Conclusions: Collectively, for the first time our studies prove that TUS inhibits osteoclastogenesis by suppressing the NF-κb and p38 MAPK signaling pathways, therefore serving as a potential natural compound to treat periprosthetic osteolysis-induced aseptic prosthetic loosening.

Background

Skeleton system bears body weight and supports body shape with its rigidity, while the normal metabolism of bone tissue relies on a dynamic balance between generation and resorption mediated by the osteoblast and osteoclast respectively [1, 2]. In the contrary, the pathological generation of osteoclast is discovered as the “culprit” of various orthopedic disorders manifesting as bone loss or osteolysis, like aseptic prosthetic loosening of artificial joint, postmenopausal osteoporosis and bone metastasis of some cancers [3–5], which produce poor prognosis and demanding healthcare reqiurement. Especially, inflammatory cytokines and chemokines induced osteoclast generation seems to be a major cause of

periprosthetic osteolysis [6]. Given the situation, exploitation in therapeutical treatment against osteoclast over-production show great significance in the clinical management of aseptic prosthetic loosening.

Osteoclast is a type of highly-differentiated multi-nuclear giant cell comprised of fused monocyte-macrophage progenitors originating from hematopoietic lineage [7], like bone marrow macrophages (BMMs) and RAW264.7. Much works have been done to unravel molecular mechanism of osteoclastogenesis and several canonical pathway come to be clear. As a leading pro-osteoclastogenesis factor, the receptor activator of nuclear factor kB ligand (RANKL) initiates a primary signal by binding to RANK locating in the membrane to activate TNF receptor-associated factor 6 (TRAF 6) [8]. TRAF 6 plays a pivotal role in the promotion of PI3K-Akt, NF-κB and MAPK signaling pathways (including JNK, ERK and p38 pathways) via up-regulating the Src, IkB kinase (IKK) complex and MEK/MKK respectively [9–11]. CaMK-CREB and Jak-STAT also participates to regulate the transcription process of osteoclastic bone resorption [12, 13]. Activation of these cascades are proven to be responsible for the increase in expression of specific genes, like Cathepsin K, tartrate-resistant acid phosphatase (TRAP), c-Fos and cytoskeletal rearrangement during the macrophages fusion [14, 15], which regulates the bio-function of osteoclasts. Hence, agents targets canonical pathways like NF-κB and MAPK may promise an effective anti-osteoclastogenesis property in the management of aseptic prosthetic loosening.

Tussilagone (TUS) is a type of sesquiterpenoids that was isolated from the flower of Tussilago Farfara or some other species in the genus Tussilago. Previous studies suggested that this natural compound exerts therapeutical effects in inflammatory pulmonary diseases[16], inflammatory intestinal diseases (IBD)[17], ischemic stroke[18], colon cancer[19], obesity and type 2 diabetes[20], demonstrating multiple regulatory characteristics in diverse pathophysiological changes like anti-inflammation[21–23], anti-oxidation[24, 25], anti-tumor[19]. Especially, TUS was found attenuating lipopolysaccharide (LPS)-induced inflammatory mediators production in RAW264.7 cell via NF-κB and (or) MAPK signaling cascades in several studies[21–23], therefore may falling in the candidates of possible drugs to protect bone by suppressing osteoclast formation and activation. However, except for the mentioned effects towards osteoclast progenitors and other cell lines, few understanding is known about whether and how TUS suppresses RANKL-induced osteoclast differentiation and improves periprosthetic osteolysis-induced aseptic prosthetic loosening in vivo. Therefore, we designed such a study to investigate the therapeutic benefits of TUS for osteoclast and illuminate the underlying molecular mechanism, thus complementing the theory and suggesting greater value of TUS in the treatment of osteolytic diseases.

Materials And Methods

Reagents and cell preparation

TUS (purity >98%, Fig. 3. A) was purchased from Dalian Meilun Biotechnology (Liaoning, China) and dissolved in alpha modification of minimum essential medium (α-MEM) at the concentration of 0.2 M as storage solution stocking at 4℃. The α-MEM medium was obtained from Gibco-BRL (Gaithersburg, MD, USA). The fetal bovine serum (FBS), penicillin /streptomycin, soluble mouse recombinant M-CSF and

RANKL were acquired from R&D Systems (Minneapolis, MN, USA). The cell counting kit (CCK-8) was obtained from Dojindo Molecular Technology (Japan) The DMSO and TRAP staining kit was obtained from Sigma-Aldrich (St. Louis, MO, USA).

RAW264.7 cells was purchased from American Type Culture Collection (Rockville, MD, USA) and were incubated in α-MEM supplemented with 10% FBS and 1% penicillin/streptomycin, namely complete α-MEM. 4 to 6 week-old C57BL/6 mice were acquired from Shanghai Laboratory Animal Company (SLACCAS, Shanghai, China). Primary BMMs were separated from the whole bone marrow of murine femurs and tibias and cultured in complete α-MEM with the addition of 30 ng/ml M-CSF. All cells we used in this study were incubated in the incubator with constant high humidity, 37 ℃ and 5% CO2 atmosphere [26]. Non-adherent cells were removed before each passage.

Cell viability

The cytotoxic effects of TUS on RAW264.7 and BMMs cells were assessed using a CCK-8 assay according to the instruction book. RAW264.7 or BMMs cells were plated in 96-well plates at a density of 3 × 10^3 cells/well for adhesion overnight. Cells were then treated with diverse concentrations of TUS (0, 0.39, 0.78, 1.56, 3.13, 6.25, 12.5, 25, 50 or 100 uM) for 48 h or 96 h. A 10 μl volume of CCK-8 buffer was added to each well, and cells were incubated at 37 ℃ for an additional 1 h. Then, the optical density (OD) was detected at a wavelength of 450 nm (650 nm reference) on an ELX800 absorbance microplate reader (Bio-Tek, USA). Cell viability was calculated relative to control using the following formula: (experimental group OD - zeroing OD)/(control group OD - zeroing OD) [27].

Osteoclast formation assay

To investigated the effect of TUS on osteoclast formation *in vitro*, RAW264.7 or BMMs cells were seeded in 96-well plates respectively at a density of 2.5×10^3 cells/well and then cultured for adhesion overnight. After confirming the healthy condition of the cells, they were cultured with complete α-MEM with 50 ng/mL of RANKL (30 ng/mL of M-CSF for BMMs cells solely) and different non-cytotoxic concentrations of TUS (0, 6.25, 12.5, 25 uM), until osteoclast formation was clearly observed 5 days later. The osteoclasts were fixed with 4% paraformaldehyde for 20min and then stained for TRAP. TRAP-positive cells with more than five nuclei were counted as osteoclasts.

Bone resorption pit evaluation

RAW264.7 cells were plated onto the surface of sterile bovine bone slices in 96-well plates at a density of 3×10^3 cells/well and then cultured complete α-MEM containing 50 ng/mL of RANKL (30 ng/mL of M-CSF for BMMs cells solely) and different concentrations of TUS (0, 6.25, 12.5, 25 uM). After confirming osteoclast formation, the cells were treated with complete culture medium supplemented with 30 ng/mL of M-CSF, 50 ng/mL of RANKL, and different TUS concentrations for another 48 h. Finally, bone resorption effect on the bovine bone slices was evaluated using scanning electron microscope (SEM; FEI Quanta 250).

RNA extraction and quantitative PCR analysis

Quantitative PCR was applied to measure the expression of osteoclast specific genes. We seeded BMMs in 24-well plates at a density of 1×10^5 cells/well and treated them with complete α-MEM, 50 ng/ml RANKL and 30 ng/ml M-CSF. Cells were administered with different concentrations of TUS (0, 6.25, 12.5 or 25 uM). Then, we extracted RNA with the Qiagen RNeasy Mini kit (Qiagen, Valencia, CA, USA) according to the instruction book. Next, we synthesize cDNA from 1 mg of total RNA using reverse transcriptase kit (TaKaRa Biotechnology, Otsu, Japan). The SYBR Premix Ex Tag kit (TaKaRa Biotechnology) and an ABI 7500 Sequencing Detection System (Applied Biosystems, Foster City, CA, USA) was used in qPCR. PCR conditions were 40 cycles of denaturation at 95 °C for 5s and amplification at 60 °C for 34s [26]. The reactions were conducted in triplicate. The mice primer sequence set is listed in Table 1.

NF-κB luciferase reporter gene assay

To examine whether TUS affected NF-κB gene expression, RAW264.7 cells were stably transfected with a p-NF-κB-TA-Luc luciferase reporter construct. Concisely, cells were plated in a 24-well plate at a density of 1×10^5 cells/well. 24 hours later, cells were pre-treated with different concentrations of TUS (0, 6.25, 12.5, 25 uM) for 1 h, prior to incubation with 50 ng/mL RANKL for another 8 h. Cells were then lysed and luciferase activity was measured using the Promega Luciferase Assay System according to the instruction book [15].

Western blotting analysis

We seeded RAW264.7 cells in 6-well plates at a density of 5×10^5 cells/well. When the cells were confluent, they were pre-treated with or without 25 uM TUS for 4 h. Cells were then incubated with 50 ng/mL RANKL for 0, 5, 10, 20, 30, or 60 min. Total proteins were extracted from cultured cells using radioimmunoprecipitation assay (RIPA) lysis buffer (Well Biology, Changsha, China) with protease inhibitor cocktail. Next, the lysates were centrifuged at 12,000 g for 15 min, and the supernatants that contained the proteins were collected. Protein concentrations were measured with bicinchoninic acid assay (Well Biology).

We resolved 30 mg of each protein lysate using sodium dodecyl sulfatepolyacrylamide gel electrophoresis (SDS-PAGE) on 10% gels, and transferred products to polyvinylidene difluoride (PVDF) membranes. Following transfer, membranes were blocked with 5% skimmed milk powder in TBS-Tween (TBS: 0.05 M Tris, 0.15 M NaCl, pH 7.5, and 0.2% Tween-20) for 1 h, and then incubated with primary antibodies overnight at 4 ℃ [15]. Membranes were then rinsed with TBS-Tween and incubated with the corresponding secondary antibodies conjugated with IRDye 800CW (molecular weight 1162 Da) for 2 h. Bands were detected through the Odyssey infrared imaging system (LI-COR Bioscience, Lincoln, NE, USA). Quantitative analysis of bands' intensity was performed by image J software.

Titanium particle-induced calvarial osteolysis model

Protocols for this study is censored by the Medical Ethics Committee of the Second Xiangya Hospital, Central South University and all experiment procedures were performed in accord with the related recommendations of guiding principles.

We established a murine calvarial osteolysis model to determine the preventative effects of TUS on osteolysis *in vivo*. In short, 16 healthy 8-week-old C57BL/6 mice (weight: 21.47 ± 1.22 g) were bred in specific pathogen-free (SPF) plastic-isolator cages assigned randomly into 3 groups: sham PBS control (sham), titanium (Ti) particles with PBS (vehicle), and Ti particles with 10 mg/kg/day of TUS (TUS group). To remove endotoxins adherent on Ti particles, commercial pure Ti particles were sterilized by baking at 180 ℃ for 6 h, followed by treatment of 70% ethanol for 2 days. The murines were anesthetized, and the cranial periosteum was separated from the calvarium by sharp dissection. Then, 30 mg of Ti particles were planted under the periosteum at the middle suture of the calvarium [15]. Mice in TUS group were injected intraperitoneally with TUS at 10 mg/kg/day for 8 weeks. Mice in the sham and vehicle groups received PBS daily. At the end of the experiment, the mice were sacrificed, and the calvaria were excised and fixed in 4% paraformaldehyde for micro-computed tomography (CT) analysis.

Micro CT scanning

The fixed calvaria were observed using a high-resolution micro-CT system (μCT50, Scanco, Switzerland). The scanning protocol was set at an isometric resolution at 8.3 mm, and X-ray energy settings of 80 kV and 80 mA. After reconstruction, a square ROI around the midline suture was selected for further qualitative and quantitative analysis. BV/TV, the number of porosity and percentage of total porosity of each sample were analyzed.

Histomorphometric analysis

After micro-CT scanning, the calvaria samples were decalcified in 10% ethylene diamine tetraacetic acid (EDTA) for 3 weeks, and then embedded in paraffin. Histological sections were preconditioned for TRAP and hematoxylin and eosin (H&E) staining. The specimens were then examined and photographed under a high quality microscope. The number of TRAP-positive multinucleated osteoclasts was counted in each sample.

Statistical analysis

The data were expressed as means ± SD. Results were analyzed using Student's t-test using the SPSS 13.0 software (SPSS Inc., USA). $P < 0.05$ indicated a significant difference between groups.

Results

TUS alleviates titanium particle-induced osteolysis in mice

TUS was previously proved to alleviate LPS-stimulated inflammatory reaction in RAW264.7 and cecal ligation and puncture (CLP)-induced septic murine model by down-regulating NF-κB and MAPK pathways

[22]. Whereas osteoclast over-activated by aseptic inflammation is also a main factor of osteoclast-dominated osteolytic diseases like aseptic prosthetic loosening. Thus, we carried out an animal experiment in Ti particle-induced murine calvarial osteolysis model to investigate the anti-bone-resorption bioactivity of TUS. Micro-CT with three-dimensional reconstruction demonstrated intensive bone resorption in the vehicle group compared to the sham group, while reduced particle-induced osteolysis is observered in the TUS treatment group (Fig. 1. A). The measurements of bone volume/total volume (BV/TV), number of porosity and the percentage of total porosity in the region of interest witnessed evident osteolysis induced by Ti particles in vehicle group. In the 10 mg/kg/day TUS treatment group, osteolysis was significantly attenuated compared to the vehicle group. (Fig. 1. B).

Histomorphometric analysis further confirmed anti-bone-resorption effect mediated by TUS. The presence of Ti particles induced the inflammatory infiltration of lymphocytes and macrophages, as well as multinucleated osteoclasts at the injection site. TRAP staining revealed that multiple osteoclasts lined along the eroded bone surface in Ti group. Corroboratively, the roughness and area of erosion surface reduced in the TUS treatment groups, with the number of TRAP-positive osteoclast decreased. (Fig. 2.)

TUS suppresses osteoclastogenesis and bone resorption function at non-cytotoxic concentration in vitro

After confirming anti-osteolysis effect of TUS *in vivo*, we directly testified the influence of TUS at various concentrations on osteoclast differentiation at cell level. Numerous TRAP-positive mature multinucleated giant cells derived from RAW264.7 or BMMs in the control group were clearly recognized. Whereas, the size and number of TRAP-positive mature multinucleated giant cells decreased as the concentration of TUS gradually increased, which indicated TUS exerted inhibitory effect on osteoclast formation in a dose-dependent manner. (Fig. 3. B and C)

Furthermore, we supposed that bone resorption function of osteoclasts are down-regulated by TUS. SEM visualization demonstrated that TUS groups presented less, smaller and shallower resorption pits relative to control group. (Fig. 4.)

To diminish the possible influence of cytotoxicity, we determine the cytotoxic concentration threshold of TUS using a CCK-8 assay. We discovered that pre-treatment of TUS equal or less than 25 uM show no suppressive effect in BMMs or RAW264.7 assays. (Fig. 3. B and C) Collectively, our data suggest that TUS mitigates osteoclast bone resorption *in vitro*.

TUS inhibits the expression of osteoclast-specific genes

Since osteoclast differentiation is accompanied with RANKL-induced excessive expression of particular genes, we tried to map out the alternation of them after TUS preconditioning using qPCR. We found that mRNA expression of osteoclast-specific genes, including NFATc1, Calcr, TRAF6, c-Fos, DC-STAMP and Cathepsin K culminated in response to RANKL stimulation in the control group .However, TUS hindered the transcription of these genes in a dose-dependent manner. (Fig. 5.) These data prove that TUS suppresses osteoclastogenesis by attenuating osteoclast specific gene expression *in vitro*.

TUS hinders RANKL-induced activation of NF-κB and p38 signaling pathways

As mentioned before, NF-κB and MAPK are two major pathways in the osteoclatogenesis signaling cascade, so we attempted to elucidate the mechanism underlying the anti-osteoclastogenesis effect of TUS by detecting the signal molecules in NF-κB and MAPK pathways using western blotting. The upstream RANKL-induced phosphorylation of IKK complex, as we mentioned before, activates the following signaling cascades of NF-κB and MAPK pathways. IκBα, the inhibitory unit used to bind with NF-κB, disassociates from the location and degrades after being phosphorylated, which leads to the nuclear translocation of subunit p65 and the next signaling procedures. The analysis of bands shown that the quantity of IκBα at 5, 10 min was significantly impaired by TUS treatment (Fig. 6. B and C). For more, the suppressive effect of TUS in NF-κB signaling pathway was further supported by the analysis of NF-κB luciferase reporter gene assay (Fig. 6. A) Also, the the whole span of 60 min witnessed an extensive cutting down of p-p38 level at each time caused by TUS administration (Fig. 6. B and C).

Apart from this, no obvious alteration was detected in the expression of JNK/P-JNK and ERK/p-ERK with or without TUS treatment.

Collectively, the consequences indicated that TUS targets the degradation of IκBα and phosphorylation of p38, therefore inhibiting RANKL-mediated NF-κB and MAPK signaling activation.

Discussion

Periprosthetic osteolysis caused aseptic prosthetic loosening has been considering as the main factor of failure in joint replacement surgery. When it comes to the resorts to cope with periprosthetic osteolysis, limited surgical treatment choice like complete or partial revision with bone grafting of joint replacement are far from satisfactory because of the recurrence of osteolysis [28]. The development of orthopedics material, like highly cross-linked polyethylene (stabilized with vitamin E or not) for acetabular lining, exerts uncertain effect in the control of osteolysis compared to ultrahigh-molecular-weight polyethylene(UHMWPE)[29, 30].

As for pharmacological treatments, the benefits of existing drugs for bone protection seem to be more promising but with considerable adverse effects. Bisphosphonates function by inhibiting the expression of inflammatory mediators and impair osteoclast activity [31], but complications including osteonecrosis of the jaw (ONJ), hypocalcaemia and renal injury cause latent risks to patients [32–34]. Denosumab, a humanized monoclonal antibody, specifically combines with RANKL and down-regulates RANKL/RANK signaling [35] and shares similar adverse effects with bisphosphonates, like ONJ, hypocalcaemia, etc [36–38]. TNF-α antagonist like Infliximab hinder the osteoclastogenesis via decreasing, theoretically or actually, RANKL, TNF-α and M-CSF production [39, 40], while skin irritation like psoriasis and eczema are observed. Hence, exploitation of alternatives for anti-osteoclastogenesis drug with higher cost-effectiveness and less adverse effects are still of great significance.

So far, a great many of natural extracts have gained ground in the management of periprosthetic osteolysis [41–43] due to identical biological safety testified in the longevity of traditional Chinese medicine (TCM) and affordable prices. Tussilago Farfara is one of the most commonly used herbal medicines in East Asian and European traditional medicine for treating cough or asthma. TUS, as the main component of Tussilago Farfara, was firstly described with anti-platelet-aggregation and cardiovascular-respiratory stimulating effects in early researches published in 1980s [44, 45]. In recent years, several studies proved its beneficial effect in the treatment of diseases like diabetic obesity [20], cancers [19] and various inflammatory diseases [16–18, 22, 23]. Additionally, some scholars dedicated their studies to the metabolic patterns and parameters of TUS and set a foundation for further systematic research in patients [46–48].. In terms of molecular mechanism, the majority of retrieved literatures indicated that TUS suppresses exogenous-agent-stimulated inflammation by downregulating NF-κB signaling in different samples including human colonic tissues, airway epithelial cells, dendritic and microglial cells [16–18, 24]. Some scholars reported that TUS may repress the MAPK signaling (including JNK, ERK and p38 pathways) and then decrease production of inflammatory mediators in different cell lines and animal models [18, 22]. In addition, TUS was proven regulating cancer cell proliferation, angiogenesis an inflammation via Wnt, VEGFR2, Irf and heme oxygenase-1 (HO-1) pathways respectively [19, 24, 49]. However, whether TUS would have a suppressive effect on osteoclastogenesis via similar patterns and how it works exactly remains elusive. Therefore, we design such a study to figure it out and attempt to elucidate the possible mechanism.

In our work, TUS significantly attenuates multiple index according to micro-CT analysis of bone loss in titanium particle-induced murine calvarial osteolysis model. Immunohistochemical staining analysis witnesses an obvious drop in the number of osteoclast in gross and microscopic specimens after TUS pre-treatment compared to the control. Then, osteoclast differentiation and bone slices resorption assays come to reduction in not only the number but also the aggregate biological function caused by TUS at non-toxic concentration in a dose-dependent manner, which verify the anti-osteoclast characteristic of it. The report of qPCR that the expression of osteoclast specific genes including NFATc1, Calcr, TRAF6, c-Fos, DC-STAMP and Cathepsin K decreases in treated group also add to the validity of the consequence. Finally, we resorted to Western blotting and unearthed that TUS inhibits RANKL-induced osteoclast formation by down-regulating the NF-κB and p38/MAPK signaling pathways.

RANKL, one of the key cytokines in monocyte-macrophage lineage, is indispensable for the initiation of osteoclastogenesis and maturation of osteoclasts in vivo and in vitro [50]. The specific combination between RANKL and cytomembrane-docking RANK triggers the binding of TNFR-associated cytoplasmic factors (TRAFs) to the cytoplasmic domain of RANK, consequently producing the preliminary signal for following cascades [51]. Then, such RANKL/RANK/TRAFs complex recruits TGF-β-activated kinase 1 (TAK1), together with the TAK1 binding protein 2 (TAB2) [2, 51]. For one, TAK1 activates the phosphorylation of IKK complex and sequentially induces the breaking-free of NF-κB from inhibitive protein IκBα[52], which cause the degradation of IκBα and the translocation of p65 from NF-κB to the nuclear [1]. For another, the phosphorylation of p38 following the TAK1 activation also plays a role in the signaling induced by RANK-RANKL combination. In all, both of NF-κB and p38 signaling could trigger

sufficient expression of downstream osteoclast specific genes like Cathepsin K, TRAP, CTR, β3 integrin, c-Fos, leading to a decrease in bone resorption function eventually [53]. Herein, we adopt titanium particle-induced murine calvarial osteolysis model to explore the bioactivities of TUS in vivo. Significant osteolysis are witness in vehicle group compared to the control whereas a much more appeased situation in TUS group. The analysis of western blotting suggest the degradation of IκBα and phosphorylation of p38 apparently diminishes in TUS-treated group relative to control group. To sum up, we come to a cheerful conclusion that TUS suppresses RANKL-induced osteoclastogenesis by blocking NF-κB and p38-mediated MAPK signaling without affecting JNK and ERK pathways (Fig. 7.) in a dose-dependent manner, which is verified in animal, cell and molecular level.

However, several limitations blemish our research.

For one, the mice, as we applied in this study, has limited cancellous bone, body volume and short lifespan, thus fail to simulate the coexistence of cancellous and cortex bone, decades of wearing period causing long-term inflammatory bio-scene in human body [54], and hardly provided sufficient in-vivo space and exercise load for implants in studies of their biomechanical properties.

For another, titanium particle-induced calvarial osteolysis model, as we used, under-represents the wear-debris-induced osteolysis model used in the emulation of aspetic prosthetic loosening pathogenesis. Different types of wear particle found in the bone-graft interface of patients with different implant materials, such as titanium [55], cobalt-chromium-molybdenum (CoCrMo) [56], ceramics [54], tricalcium phosphate (TCP) [57], polyether-ether-ketone (PEEK) [58], highly cross-linked polyethylene (HXLPE) and ultrahigh-molecular-weight polyethylene(UHMWPE)[59] demonstrate various traits in osteolysis.

For more, the effect of TUS in osteoblast which also participates in the pathogenesis of aseptic prosthetic loosening [60] is not detected in our research. And only single dose concentration of TUS treatment was investigated in animal experiment. Whether in fact TUS exert anti-osteolysis effect in vivo in a dose-dependent manner need further examination. Therefore, the gradient concentration group in osteoclast and osteoblast cell models will be set in following study.

In the western blotting part, we only investigated the involvement of two classical signaling cascades, NF-κB and MAPK pathways since no record about PI3k-Akt, CaMK-CREB or other pathway closely engaged in the mechanism network of osteoclastogenesis was retrieved from the literature search. However, these uncharted patterns possibly responsible for bioactivity of TUS may require elucidation.

Our work demonstrated TUS suppresses RANKL-induced NF-κB signaling in osteoclastogenesis from RAW264.7 via modulating IκBα degradation without any obvious effect on phosphorylation of IκBα or IKK complex. Comparatively, most of previous studies suggested that TUS suppresses the activation of NF-κB pathway, while the modulated targets vary. Cheon et al. [17], Choi et al. [16], Hwang et al. [18], Kim et al. [22], Lee et al. [23] and Lim et al. [61] all reported that TUS blocks NF-κB pathway in exogenous-agent-induced colitis mice, airway epithelial cells, focal cerebral ischemia rats, septic mice, skin inflammation mice, BV-2 microglial cells by attenuating the nuclear translocation of p65 subunit, the phosphorylation

and (or) degradation of IκBα. Among them, Choi et al. [16] also observed the alleviated the phosphorylation IKK complex.

Furthermore, we suggested that TUS blocks the p38 cascades without affecting other MAPK signaling pathways, which is partially responsible for inhibited osteoclast differentiation after TUS treatment. However, Hwang et al. [18] and Kim et al. [22] demonstrated that TUS reduces MAPK signaling via inhibiting the phosphorylation of not only p38 but also JNK and ERK in focal cerebral ischemia rats and septic mice. Even, in the research of Hwangbo et al. using MAPK-inhibiting assay, an conclusion can be drawn that TUS cannot modulate MAPK pathways in nuclear factor-erythroid 2-related factor (Nrf2)/HO-1 protein production in RAW264.7, which is just opposite to our and other mention authors' theories. We believe the possible reason of the different understanding concerning the molecular mechanism of TUS treatment may lie in the different agents, cell lines and animal species used in the establishment of models. What's more, undetected crosstalkings between signal pathways can cover up the suppressed upstream molecules and mislead scholars into pathways where downstream targets locate. Hence, further studies unraveling the entire mechanism network and details of TUS bioactivities are required.

Conclusion

In summary, for the first time we discovered that TUS can attenuate osteolysis severity in titanium particle-induced murine calvarium model and verified its anti-osteoclastogenesis and anti-resorption effect in cell level. According to qPCR and western blotting analysis, these bio-activities may result from the suppression of RANKL-mediated NF-κB and p38-mediated MAPK signaling pathways. Our theory complement the therapeutic effect TUS in bone-loss osteopathies via regulating osteoclasts and broaden the spectrum of anti-osteolysis natural compounds, which promises novel potential agents in the treatment of aseptic prosthetic loosening. Still, full investigation of TUS targets and more evidence are needed for the anti-osteolysis clinical adoption.

Declarations

Ethics approval and consent to participate

All animal procedures and experimental protocols were approved by the Institutional Animal Care and Use Committee of Central South University. All samples were encoded to protect patient confidentiality. All patients signed an informed consent form, which was approved by the Institutional Review Board of the Human Subject Research Ethics Committee of Central South University, Changsha, China.

Consent for publication

Not applicable.

Funding

This work was funded by the National Natural Science Foundation of China (Grant number 81702670), the Science & Technology Department of Hunan Province (Grant number 2017WK2062), the Natural Science Foundation of Hunan Province, China (Grant No. 2018JJ2565) and the Natural Science Foundation of Hunan Province for Youths (Grant number 2019JJ50883).

Competing interests

The authors declare no conflict of interests.

Authors' contributions

The study was designed by ZO and XH. All procedures was conducted under the quality control of Panel of Laboratory of Osteopathy (DP etc.) XH carried out literature retrieval, cell studies, participated in animal studies and drafted the manuscript. GJ and SL were in charge of item procurement and participated in cell culture. DY was in charge of animal treating and sample collection. ZO and ZY provided laboratory technique support. ZC and ZL served as advisor of statistics method and application. DP and XC was was responsible for clinical context inquiry. All authors revised the article critically for intellectual content. All authors read and approved the final manuscript.

Author information

Dan Peng is the director of Laboratory of Osteopathy of at The Second Xiangya Hospital of Central South University.

Zhengxiao Ouyang is an Associated Researcher at The Second Xiangya Hospital of Central South University whose research interests center around the bone and soft tissue sarcoma and pharmacology. Zhengxiao Ouyang has received several research grants from the National Nature Science Foundation of China.

Acknowledgements:

Not applicable.

Abbreviations

BMMs: Bone marrow macrophages; BV: Bone volume; CCK-8: Cell counting kit-8; OD: Optical density; CoCrMo: Cobalt-chromium-molybdenum; CT: Computed tomography; EDTA: Ethylene diamine tetraacetic acid; FBS: Fetal bovine serum; GLP-2: Glucagon-like peptide 2; HO-1: Heme oxygenase-1; M-CSF: Macrophage colony-stimulating factor; MMP: Matrix metalloproteinases; Nrf: Nuclear factor-erythroid 2-related factor; ONJ: Osteonecrosis of the jaw; OVX: Ovariectomized; PBS: Phosphate buffer solution; PEEK: Polyether-ether-ketone; PMMA: Polymethyl methacrylic; qPCR: Quantative polymerase chain reaction; RANKL: Receptor activator of nuclear factor kB ligand; SD: Standard deviation; SDS-PAGE: Sodium dodecyl sulfatepolyacrylamide gel electrophoresis; SEM: Scanning electron microscope; TBS:

Tris buffer solution; TCP: Tricalcium phosphate; Ti: Titanium; TRAP: Tartrate-resistant acid phosphatase; TUS: Tussilagone; TV: Total volume; UHMWPE: Ultrahigh-molecular-weight polyethylene.

References

1. Ouyang Z, Huang Q, Liu B, Wu H, Liu T, Liu Y: **Rubidium Chloride Targets Jnk/p38-Mediated NF-kappaB Activation to Attenuate Osteoclastogenesis and Facilitate Osteoblastogenesis.***Front Pharmacol* 2019, **10:**584.
2. Zhu W, Yin Z, Zhang Q, Guo S, Shen Y, Liu T, Liu B, Wan L, Li S, Chen X, et al: **Proanthocyanidins inhibit osteoclast formation and function by inhibiting the NF-kappaB and JNK signaling pathways during osteoporosis treatment.***Biochem Biophys Res Commun* 2019, **509:**294-300.
3. Crotti TN, Smith MD, Findlay DM, Zreiqat H, Ahern MJ, Weedon H, Hatzinikolous G, Capone M, Holding C, Haynes DR: **Factors regulating osteoclast formation in human tissues adjacent to peri-implant bone loss: expression of receptor activator NFkappaB, RANK ligand and osteoprotegerin.***Biomaterials* 2004, **25:**565-573.
4. Maurizi A, Rucci N: **The Osteoclast in Bone Metastasis: Player and Target.***Cancers (Basel)* 2018, **10**.
5. Rachner TD, Khosla S, Hofbauer LC: **Osteoporosis: now and the future.***Lancet* 2011, **377:**1276-1287.
6. Goodman SB, Ma T: **Cellular chemotaxis induced by wear particles from joint replacements.***Biomaterials* 2010, **31:**5045-5050.
7. Ono T, Nakashima T: **Recent advances in osteoclast biology.***Histochem Cell Biol* 2018, **149:**325-341.
8. Asagiri M, Takayanagi H: **The molecular understanding of osteoclast differentiation.***Bone* 2007, **40:**251-264.
9. Cao H, Yu S, Yao Z, Galson DL, Jiang Y, Zhang X, Fan J, Lu B, Guan Y, Luo M, et al: **Activating transcription factor 4 regulates osteoclast differentiation in mice.***J Clin Invest* 2010, **120:**2755-2766.
10. Ping Z, Wang Z, Shi J, Wang L, Guo X, Zhou W, Hu X, Wu X, Liu Y, Zhang W, et al: **Inhibitory effects of melatonin on titanium particle-induced inflammatory bone resorption and osteoclastogenesis via suppression of NF-kappaB signaling.***Acta Biomater* 2017, **62:**362-371.
11. Wang L, Iorio C, Yan K, Yang H, Takeshita S, Kang S, Neel BG, Yang W: **A ERK/RSK-mediated negative feedback loop regulates M-CSF-evoked PI3K/AKT activation in macrophages.***Faseb j* 2018, **32:**875-887.
12. Farr JN, Xu M, Weivoda MM, Monroe DG, Fraser DG, Onken JL, Negley BA, Sfeir JG, Ogrodnik MB, Hachfeld CM, et al: **Targeting cellular senescence prevents age-related bone loss in mice.***Nat Med* 2017, **23:**1072-1079.
13. Sato K, Suematsu A, Nakashima T, Takemoto-Kimura S, Aoki K, Morishita Y, Asahara H, Ohya K, Yamaguchi A, Takai T, et al: **Regulation of osteoclast differentiation and function by the CaMK-CREB pathway.***Nat Med* 2006, **12:**1410-1416.
14. Helming L, Gordon S: **Molecular mediators of macrophage fusion.***Trends Cell Biol* 2009, **19:**514-522.

15. Liu X, Qu X, Wu C, Zhai Z, Tian B, Li H, Ouyang Z, Xu X, Wang W, Fan Q, et al: **The effect of enoxacin on osteoclastogenesis and reduction of titanium particle-induced osteolysis via suppression of JNK signaling pathway.** *Biomaterials* 2014, **35:**5721-5730.
16. Choi BS, Kim YJ, Yoon YP, Lee HJ, Lee CJ: **Tussilagone suppressed the production and gene expression of MUC5AC mucin via regulating nuclear factor-kappa B signaling pathway in airway epithelial cells.** *Korean J Physiol Pharmacol* 2018, **22:**671-677.
17. Cheon HJ, Nam SH, Kim JK: **Tussilagone, a major active component in Tussilago farfara, ameliorates inflammatory responses in dextran sulphate sodium-induced murine colitis.** *Chem Biol Interact* 2018, **294:**74-80.
18. Hwang JH, Kumar VR, Kang SY, Jung HW, Park YK: **Effects of Flower Buds Extract of Tussilago farfara on Focal Cerebral Ischemia in Rats and Inflammatory Response in BV2 Microglia.** *Chin J Integr Med* 2018, **24:**844-852.
19. Li H, Lee HJ, Ahn YH, Kwon HJ, Jang CY, Kim WY, Ryu JH: **Tussilagone suppresses colon cancer cell proliferation by promoting the degradation of beta-catenin.** *Biochem Biophys Res Commun* 2014, **443:**132-137.
20. Park HR, Yoo MY, Seo JH, Kim IS, Kim NY, Kang JY, Cui L, Lee CS, Lee CH, Lee HS: **Sesquiterpenoids isolated from the flower buds of Tussilago farfara L. inhibit diacylglycerol acyltransferase.** *J Agric Food Chem* 2008, **56:**10493-10497.
21. Hwangbo C, Lee HS, Park J, Choe J, Lee JH: **The anti-inflammatory effect of tussilagone, from Tussilago farfara, is mediated by the induction of heme oxygenase-1 in murine macrophages.** *Int Immunopharmacol* 2009, **9:**1578-1584.
22. Kim YK, Yeo MG, Oh BK, Kim HY, Yang HJ, Cho SS, Gil M, Lee KJ: **Tussilagone Inhibits the Inflammatory Response and Improves Survival in CLP-Induced Septic Mice.** *Int J Mol Sci* 2017, **18**.
23. Lee J, Kang U, Seo EK, Kim YS: **Heme oxygenase-1-mediated anti-inflammatory effects of tussilagonone on macrophages and 12-O-tetradecanoylphorbol-13-acetate-induced skin inflammation in mice.** *Int Immunopharmacol* 2016, **34:**155-164.
24. Park Y, Ryu HS, Lee HK, Kim JS, Yun J, Kang JS, Hwang BY, Hong JT, Kim Y, Han SB: **Tussilagone inhibits dendritic cell functions via induction of heme oxygenase-1.** *Int Immunopharmacol* 2014, **22:**400-408.
25. Qin ZB, Zhang J, Wu XD, He J, Ding LF, Peng LY, Li XY, Li Y, Deng L, Guo YD, Zhao QS: **Sesquiterpenoids from Tussilago farfara and their inhibitory effects on nitric oxide production.** *Planta Med* 2014, **80:**703-709.
26. Zhang Q, Tang X, Liu Z, Song X, Peng D, Zhu W, Ouyang Z, Wang W: **Hesperetin Prevents Bone Resorption by Inhibiting RANKL-Induced Osteoclastogenesis and Jnk Mediated Irf-3/c-Jun Activation.** *Front Pharmacol* 2018, **9:**1028.
27. Zhou F, Shen Y, Liu B, Chen X, Wan L, Peng D: **Gastrodin inhibits osteoclastogenesis via down-regulating the NFATc1 signaling pathway and stimulates osseointegration in vitro.** *Biochem Biophys Res Commun* 2017, **484:**820-826.

28. Adelani MA, Mall NA, Nyazee H, Clohisy JC, Barrack RL, Nunley RM: **Revision Total Hip Arthroplasty with Retained Acetabular Component.***J Bone Joint Surg Am* 2014, **96:**1015-1020.
29. Boyer B, Bordini B, Caputo D, Neri T, Stea S, Toni A: **Is Cross-Linked Polyethylene an Improvement Over Conventional Ultra-High Molecular Weight Polyethylene in Total Knee Arthroplasty?***J Arthroplasty* 2018, **33:**908-914.
30. Endo M, Tipper JL, Barton DC, Stone MH, Ingham E, Fisher J: **Comparison of wear, wear debris and functional biological activity of moderately crosslinked and non-crosslinked polyethylenes in hip prostheses.***Proc Inst Mech Eng H* 2002, **216:**111-122.
31. Wu FQ, Ye J, Wu LG: **[Inhibitory effect of zoledronate sodium on periprosthetic osteolysis induced by polyethylene particles].***Zhongguo Gu Shang* 2015, **28:**936-939.
32. Cheng L, Ge M, Lan Z, Ma Z, Chi W, Kuang W, Sun K, Zhao X, Liu Y, Feng Y, et al: **Zoledronate dysregulates fatty acid metabolism in renal tubular epithelial cells to induce nephrotoxicity.***Arch Toxicol* 2018, **92:**469-485.
33. Edwards BJ, Gounder M, McKoy JM, Boyd I, Farrugia M, Migliorati C, Marx R, Ruggiero S, Dimopoulos M, Raisch DW, et al: **Pharmacovigilance and reporting oversight in US FDA fast-track process: bisphosphonates and osteonecrosis of the jaw.***Lancet Oncol* 2008, **9:**1166-1172.
34. Peter R, Mishra V, Fraser WD: **Severe hypocalcaemia after being given intravenous bisphosphonate.***Bmj* 2004, **328:**335-336.
35. Lacey DL, Boyle WJ, Simonet WS, Kostenuik PJ, Dougall WC, Sullivan JK, San Martin J, Dansey R: **Bench to bedside: elucidation of the OPG-RANK-RANKL pathway and the development of denosumab.***Nat Rev Drug Discov* 2012, **11:**401-419.
36. Chen J, Smerdely P: **Hypocalcaemia after denosumab in older people following fracture.***Osteoporos Int* 2017, **28:**517-522.
37. Iqbal J, Sun L, Zaidi M: **Denosumab for the treatment of osteoporosis.***Curr Osteoporos Rep* 2010, **8:**163-167.
38. Otto S, Pautke C, Van den Wyngaert T, Niepel D, Schiodt M: **Medication-related osteonecrosis of the jaw: Prevention, diagnosis and management in patients with cancer and bone metastases.***Cancer Treat Rev* 2018, **69:**177-187.
39. Kim JH, Kim AR, Choi YH, Jang S, Woo GH, Cha JH, Bak EJ, Yoo YJ: **Tumor necrosis factor-alpha antagonist diminishes osteocytic RANKL and sclerostin expression in diabetes rats with periodontitis.***PLoS One* 2017, **12:**e0189702.
40. Kitaura H, Zhou P, Kim HJ, Novack DV, Ross FP, Teitelbaum SL: **M-CSF mediates TNF-induced inflammatory osteolysis.***J Clin Invest* 2005, **115:**3418-3427.
41. Meng J, Zhou C, Hu B, Luo M, Yang Y, Wang Y, Wang W, Jiang G, Hong J, Li S, et al: **Stevioside Prevents Wear Particle-Induced Osteolysis by Inhibiting Osteoclastogenesis and Inflammatory Response via the Suppression of TAK1 Activation.***Front Pharmacol* 2018, **9:**1053.
42. Xiao F, Zhai Z, Jiang C, Liu X, Li H, Qu X, Ouyang Z, Fan Q, Tang T, Qin A, Gu D: **Geraniin suppresses RANKL-induced osteoclastogenesis in vitro and ameliorates wear particle-induced osteolysis in**

mouse model.*Exp Cell Res* 2015, **330:**91-101.

43. Zhao S, Sun Y, Li X, Wang J, Yan L, Zhang Z, Wang D, Dai J, He J, Wang S: **Scutellarin inhibits RANKL-mediated osteoclastogenesis and titanium particle-induced osteolysis via suppression of NF-kappaB and MAPK signaling pathway.***Int Immunopharmacol* 2016, **40:**458-465.
44. Hwang SB, Chang MN, Garcia ML, Han QQ, Huang L, King VF, Kaczorowski GJ, Winquist RJ: **L-652,469--a dual receptor antagonist of platelet activating factor and dihydropyridines from Tussilago farfara L.***Eur J Pharmacol* 1987, **141:**269-281.
45. Li YP, Wang YM: **Evaluation of tussilagone: a cardiovascular-respiratory stimulant isolated from Chinese herbal medicine.***Gen Pharmacol* 1988, **19:**261-263.
46. Cheng X, Liao M, Diao X, Sun Y, Zhang L: **Screening and identification of metabolites of two kinds of main active ingredients and hepatotoxic pyrrolizidine alkaloids in rat after lavage Farfarae Flos extract by UHPLC-Q-TOF-MS mass spectrometry.***Biomed Chromatogr* 2018, **32**.
47. Liu YF, Yang XW, Lu W, Xin XL: **Determination and pharmacokinetic study of tussilagone in rat plasma by RP-HPLC method.***Biomed Chromatogr* 2008, **22:**1194-1200.
48. Zhang XS, Ren W, Bian BL, Zhao HY, Wang S: **Comparative metabolism of tussilagone in rat and human liver microsomes using ultra-high-performance liquid chromatography coupled with high-resolution LTQ-Orbitrap mass spectrometry.***Rapid Commun Mass Spectrom* 2015, **29:**1641-1650.
49. Li J, Peng J, Zhao S, Zhong Y, Wang Y, Hu J, Zhang C, Cheng M, Xia G, Hu Y, et al: **Tussilagone Suppresses Angiogenesis by Inhibiting the VEGFR2 Signaling Pathway.***Front Pharmacol* 2019, **10:**764.
50. Yin Z, Zhu W, Wu Q, Zhang Q, Guo S, Liu T, Li S, Chen X, Peng D, Ouyang Z: **Glycyrrhizic acid suppresses osteoclast differentiation and postmenopausal osteoporosis by modulating the NF-kappaB, ERK, and JNK signaling pathways.***Eur J Pharmacol* 2019, **859:**172550.
51. Boyle WJ, Simonet WS, Lacey DL: **Osteoclast differentiation and activation.***Nature* 2003, **423:**337-342.
52. Futosi K, Fodor S, Mocsai A: **Reprint of Neutrophil cell surface receptors and their intracellular signal transduction pathways.***Int Immunopharmacol* 2013, **17:**1185-1197.
53. Teitelbaum SL: **Bone resorption by osteoclasts.***Science* 2000, **289:**1504-1508.
54. Gibon E, Cordova LA, Lu L, Lin TH, Yao Z, Hamadouche M, Goodman SB: **The biological response to orthopedic implants for joint replacement. II: Polyethylene, ceramics, PMMA, and the foreign body reaction.***J Biomed Mater Res B Appl Biomater* 2017, **105:**1685-1691.
55. Eger M, Hiram-Bab S, Liron T, Sterer N, Carmi Y, Kohavi D, Gabet Y: **Mechanism and Prevention of Titanium Particle-Induced Inflammation and Osteolysis.***Front Immunol* 2018, **9:**2963.
56. Wang Z, Liu N, Liu K, Zhou G, Gan J, Wang Z, Shi T, He W, Wang L, Guo T, et al: **Autophagy mediated CoCrMo particle-induced peri-implant osteolysis by promoting osteoblast apoptosis.***Autophagy* 2015, **11:**2358-2369.

57. Lv S, Zhang Y, Yan M, Mao H, Pan C, Gan M, Fan J, Wang G: **Inhibition of osteolysis after local administration of osthole in a TCP particles-induced osteolysis model.** *Int Orthop* 2016, **40:**1545-1552.
58. Du Z, Zhu Z, Wang Y: **The degree of peri-implant osteolysis induced by PEEK, CoCrMo, and HXLPE wear particles: a study based on a porous Ti6Al4V implant in a rabbit model.** *J Orthop Surg Res* 2018, **13:**23.
59. Ormsby RT, Solomon LB, Yang D, Crotti TN, Haynes DR, Findlay DM, Atkins GJ: **Osteocytes respond to particles of clinically-relevant conventional and cross-linked polyethylene and metal alloys by up-regulation of resorptive and inflammatory pathways.** *Acta Biomater* 2019, **87:**296-306.
60. Granchi D, Amato I, Battistelli L, Ciapetti G, Pagani S, Avnet S, Baldini N, Giunti A: **Molecular basis of osteoclastogenesis induced by osteoblasts exposed to wear particles.** *Biomaterials* 2005, **26:**2371-2379.
61. Lim HJ, Lee HS, Ryu JH: **Suppression of inducible nitric oxide synthase and cyclooxygenase-2 expression by tussilagone from Farfarae flos in BV-2 microglial cells.** *Arch Pharm Res* 2008, **31:**645-652.

Table

Table 1

Murines primer sequence set for qPCR

Gene	Forward primer	Reverse primer
CALCR	5′-CGGACTTTGACACAGCAGAA-3′	5′-AGCAGCAATCGACAAGGAGT-3′
Cathepsin K	5′-CTTCCAATACGTGCAGCAGA-3′	5′-TCTTCAGGGCTTTCTCGTTC-3′
c-Fos	5′-CCAGTCAAGAGCATCAGCAA-3′	5′-AAGTAGTGCAGCCCGGAGTA-3′
DC-STAMP	5′-AAAACCCTTGGGCTGTTCTT-3′	5′-AATCATGGACGACTCCTTGG-3′
NFATc1	5′-CCGTTGCTTCCAGAAAATAACA-3′	5′-TGTGGGATGTGAACTCGGAA-3′
TRAF6	5′-AAACCACGAAGAGGTCATGG-3′	5′-GCGGGTAGAGACTTCACAGC-3′
GADPH	5′-ACCCAGAAGACTGTGGATGG-3′	5′-CACATTGGGGGTAGGAACAC-3′

Figures

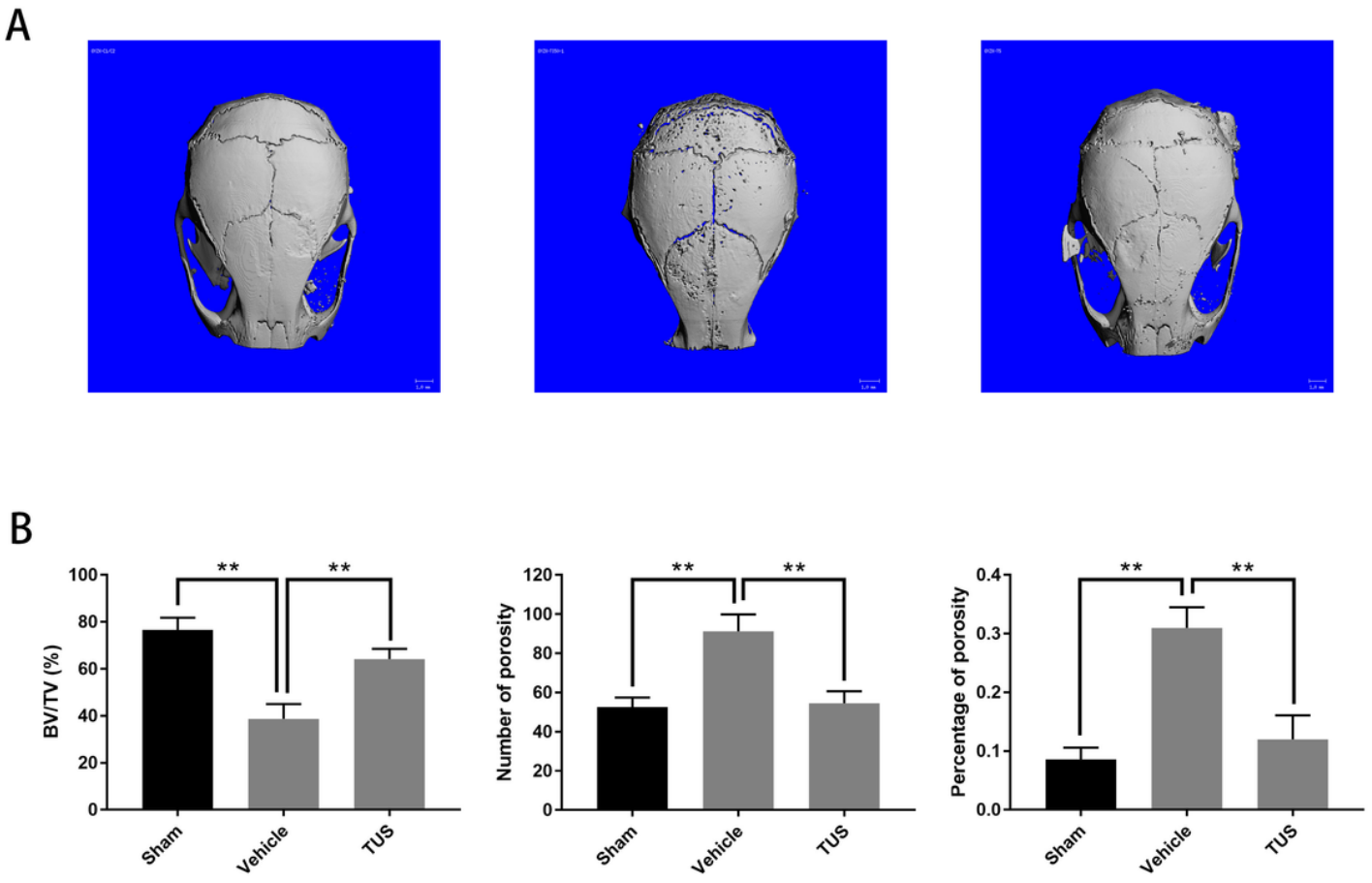

Figure 2

TUS prevented titanium particle-induced in murine calvarium osteolysis. (A) Representative three-dimensional reconstructed images of calvarium of micro-computed tomography (micro-CT) from each group. (B) Bone volume against tissue volume (BV/TV), number of porosity, and the percentage of total porosity of each sample was measured. (*: $P < 0.05$; **: $P < 0.01$ versus control group)

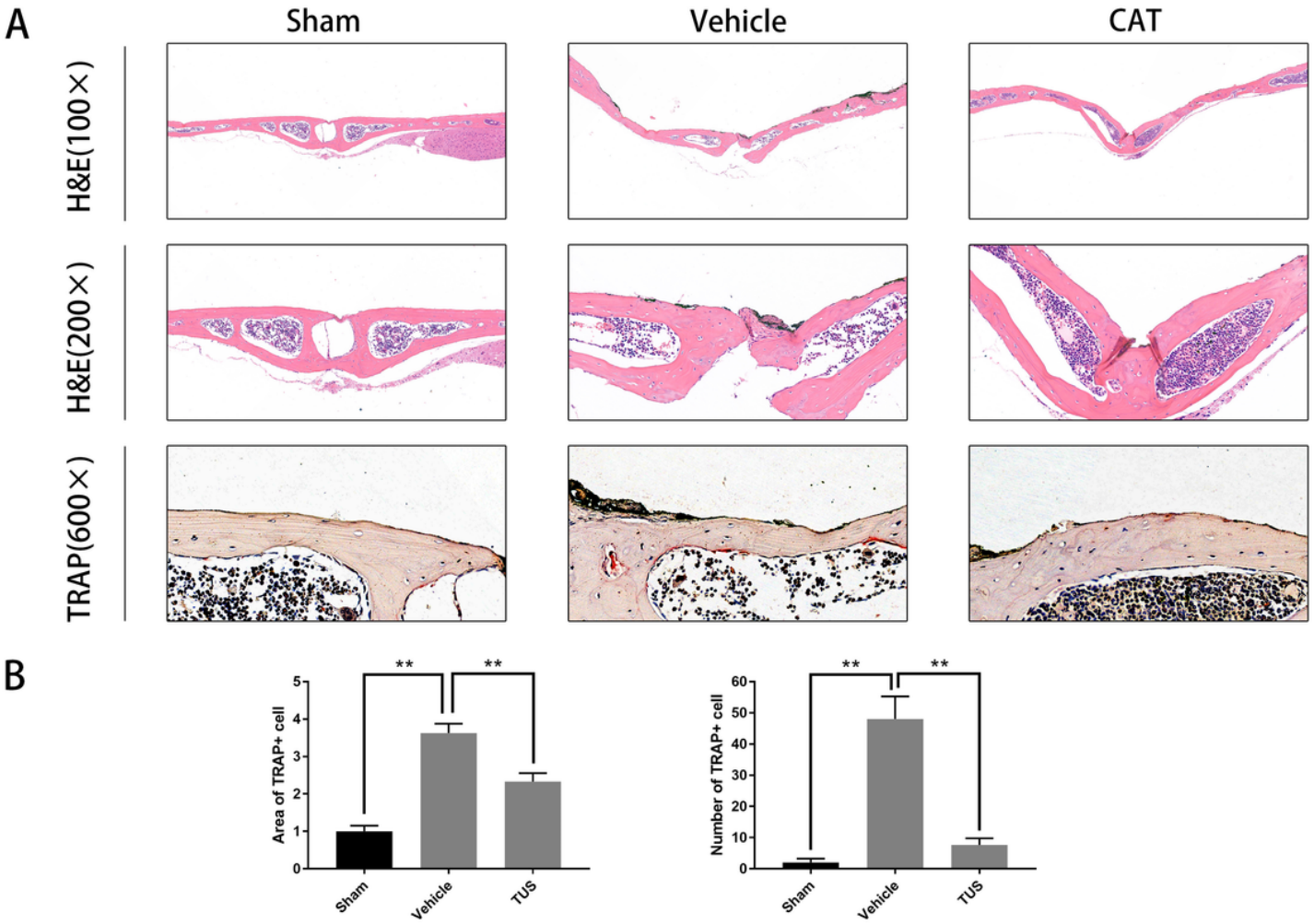

Figure 3

TUS prevented titanium particle-induced murine calvarial osteolysis assessed using immunohistochemical staining analysis. Hematoxylin and eosin (HE) and tartrate-resistant acid phosphatase (TRAP) staining were performed from at least three sections per group. The sham section showed few inflammatory and osteolytic changes. The vehicle group demonstrated an obvious inflammatory reaction and prominent osteolysis, whereas the TUS-treated groups exhibited declined inflammation and osteolysis. All experiments were performed at least three times. (*: $P < 0.05$; **: $P < 0.01$ versus control group)

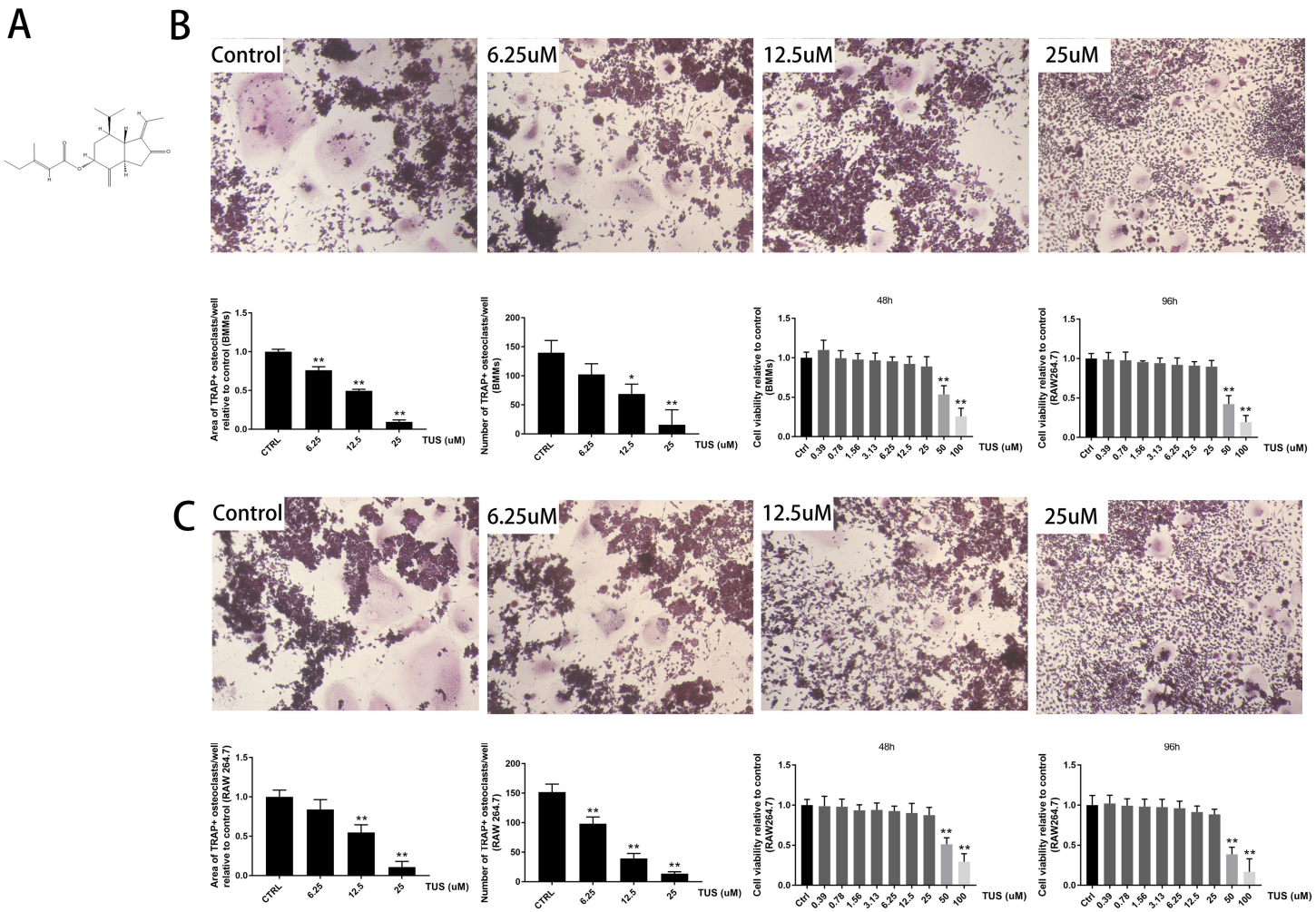

Figure 5

TUS suppressed RANKL-mediated osteoclastogenesis in a dose-dependent manner without obvious cytotoxicity in RAW264.7 cell line. (A) The structural formula of TUS. (B) BMMs were treated with various concentrations of TUS (0, 0.39, 0.78, 1.56, 3.13, 6.25, 12.5, 25, 50 or 100 uM) followed by M-CSF (30mg/ml) and RANKL (50ng/ml) stimulation for 5 days, then cells were fixed with 4% PFA and subjected to TRAP staining. Number and area of TRAP-positive osteoclasts relative to control group were quantified as described in the methods. Cell viability was determined by CCK-8 assays at 48 h or 96 h, as described in the methods. (C) RAW264.7 were treated with the same gradient concentrations of TUS as in BMMs, then, followed by RANKL (50ng/ml) stimulation for 5 days. Cells were fixed with 4% PFA and subjected to TRAP staining. Number and area of TRAP-positive osteoclasts relative to control group were quantified as described in the methods. Cell viability was determined by CCK-8 assays at 48 h or 96 h, as described in the methods. (*: $P < 0.05$; **: $P < 0.01$ versus control group)

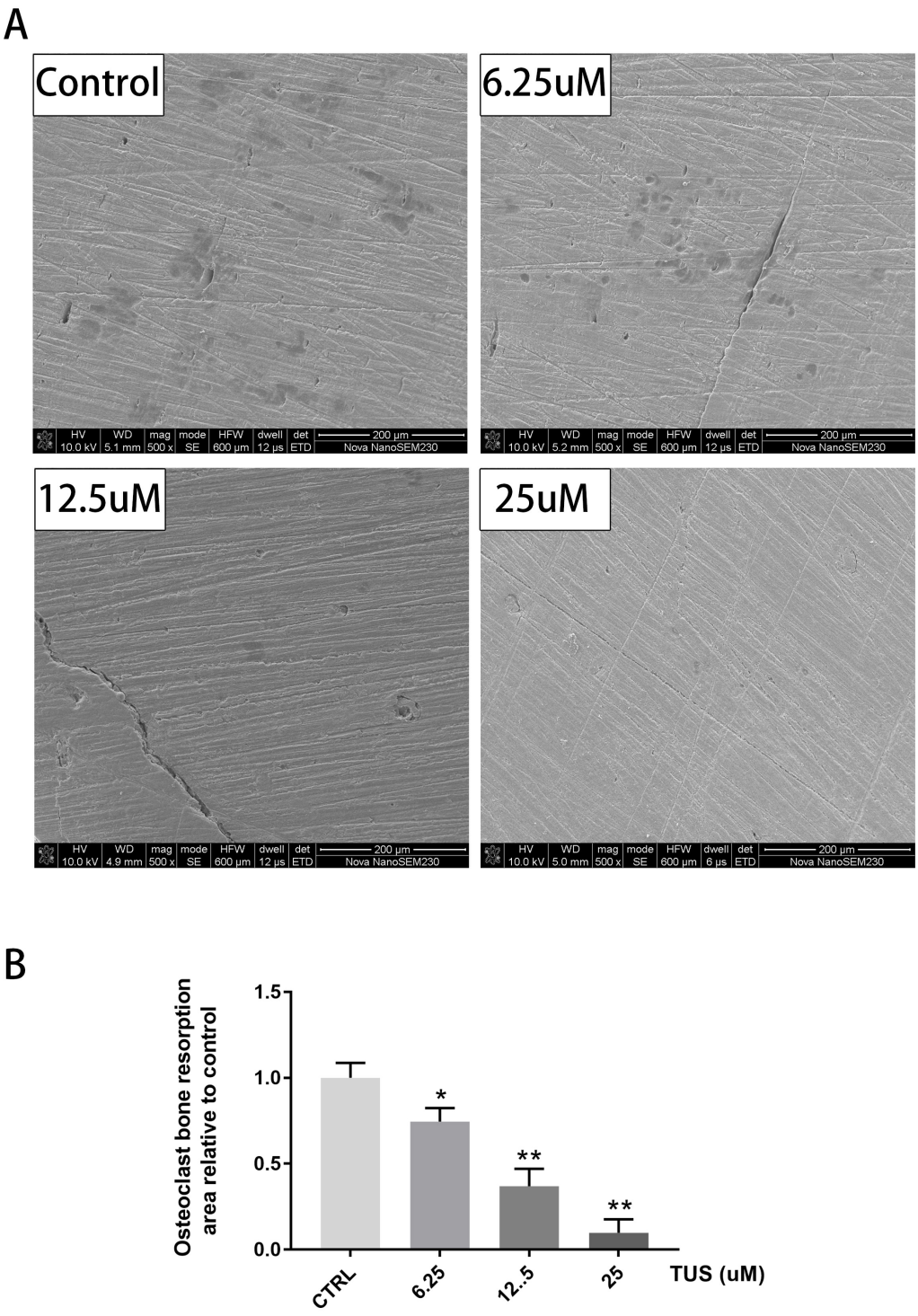

Figure 8

TUS treatment mitigated the bone resorption induced by osteoclast at non-cytotoxic concentration in a dose-dependent manner. (A) BMMs (2.5 × 103cells/well) were planted on surface of bovine bone slices and cultured with complete MEM medium, then treated with TUS at various non-cytotoxic concentrations of TUS (0, 6.25, 12.5, 25 uM), 30 ng/ml M-CSF and 50 ng/ml RANKL until visible multi-nuclear giant cell emerged in control group. Then cells were cultivated as mentioned above for another 48 h. Images under

scanning electron microscope (SEM) of all groups were present here. Bone resorption pits (white arrows) (B) Area of the bone resorption relative to control were quantified by Image J software. All experiments were performed at least three times. (*: P < 0.05; **: P < 0.01 versus control group)

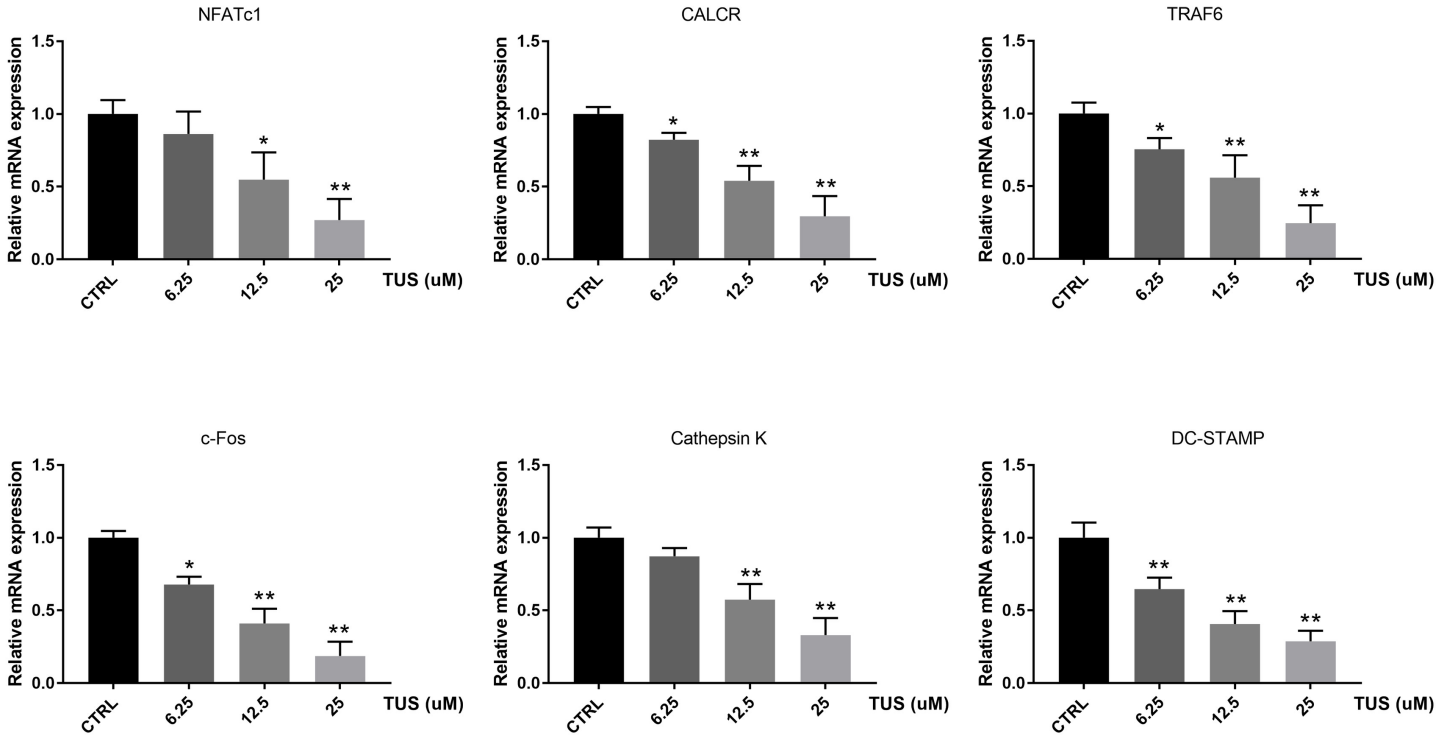

Figure 10

TUS hindered transcription of osteoclast specific genes, including NFATc1, Calcr, TRAF6, c-Fos, DC-STAMP and Cathepsin K. BMMs were cultivated with M-CSF (30 ng/ml) and RANKL (50 ng/ml) with various concentrations of TUS (0, 6.25, 12.5, 25 uM) and osteoclast-specific gene expression was analyzed by qPCR. Measured results were normalized to the expression of GAPDH. All experiments were performed at least three times. (*: P < 0.05; **: P < 0.01 versus control group)

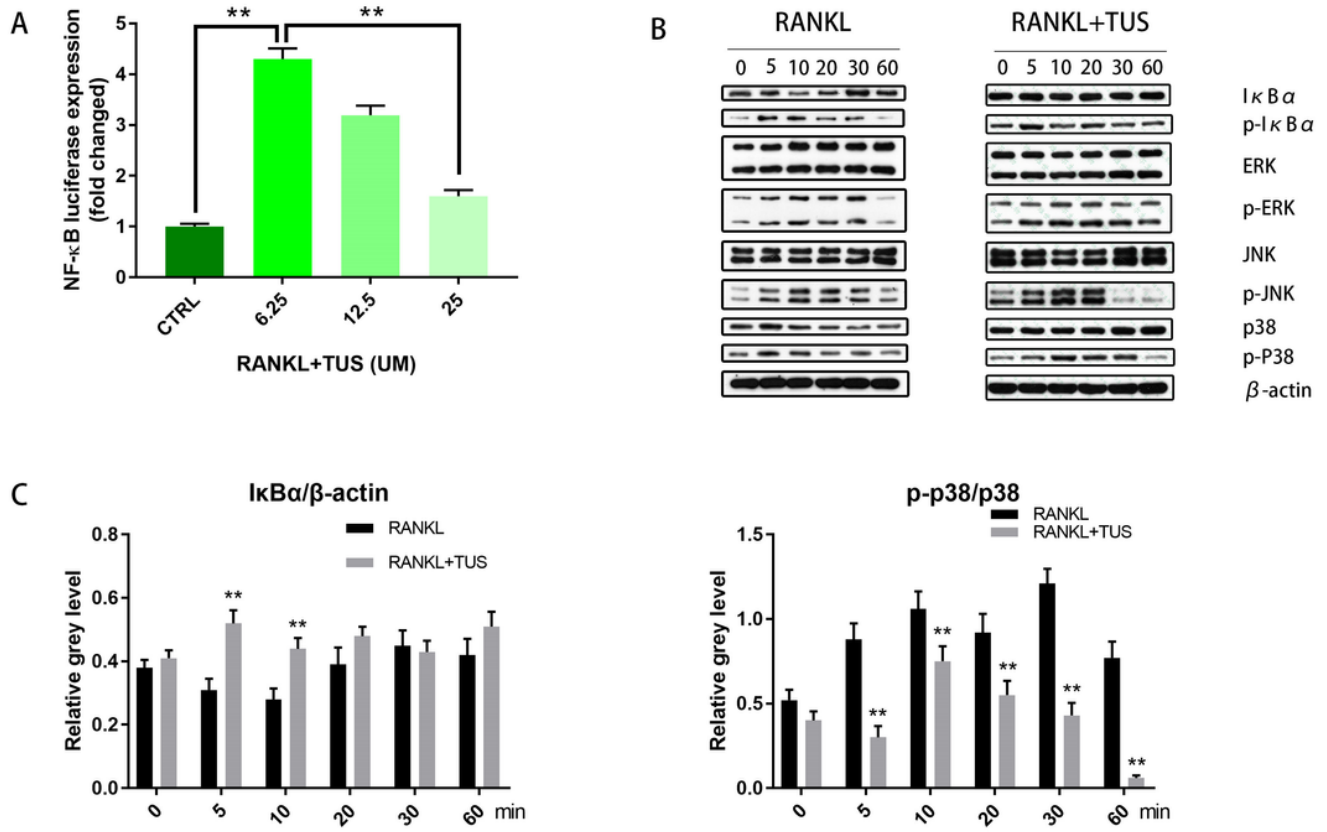

Figure 12

(A) RAW264.7 cells that were stably transfected with an NF-kB luciferase reporter construct were pre-treated with the indicated concentrations of TUS for 1 h and then incubated in the absence or presence of RANKL for 12 h. Luciferase activity was then determined using the Promega luciferase assay system. (B) TUS inhibited RANKL-induced activation of NF-κB, p38-mediated MAPK signaling pathway. RAW264.7 cells were pre-treated with or without 25 uM for 4 h. Cell lysates were analyzed by Western blotting with specific antibodies against p38, p-p38, IκBα, p-IκBα, ERK, p-ERK, JNK, p-JNK and β-actin. The band intensity was quantified using Image J software. (C) Average ratio of IκBα relative to β-actin, p-p38 relative to p38 were demonstrated. All experiments were performed at least three times. (*: $P < 0.05$; **: $P < 0.01$ versus control group)

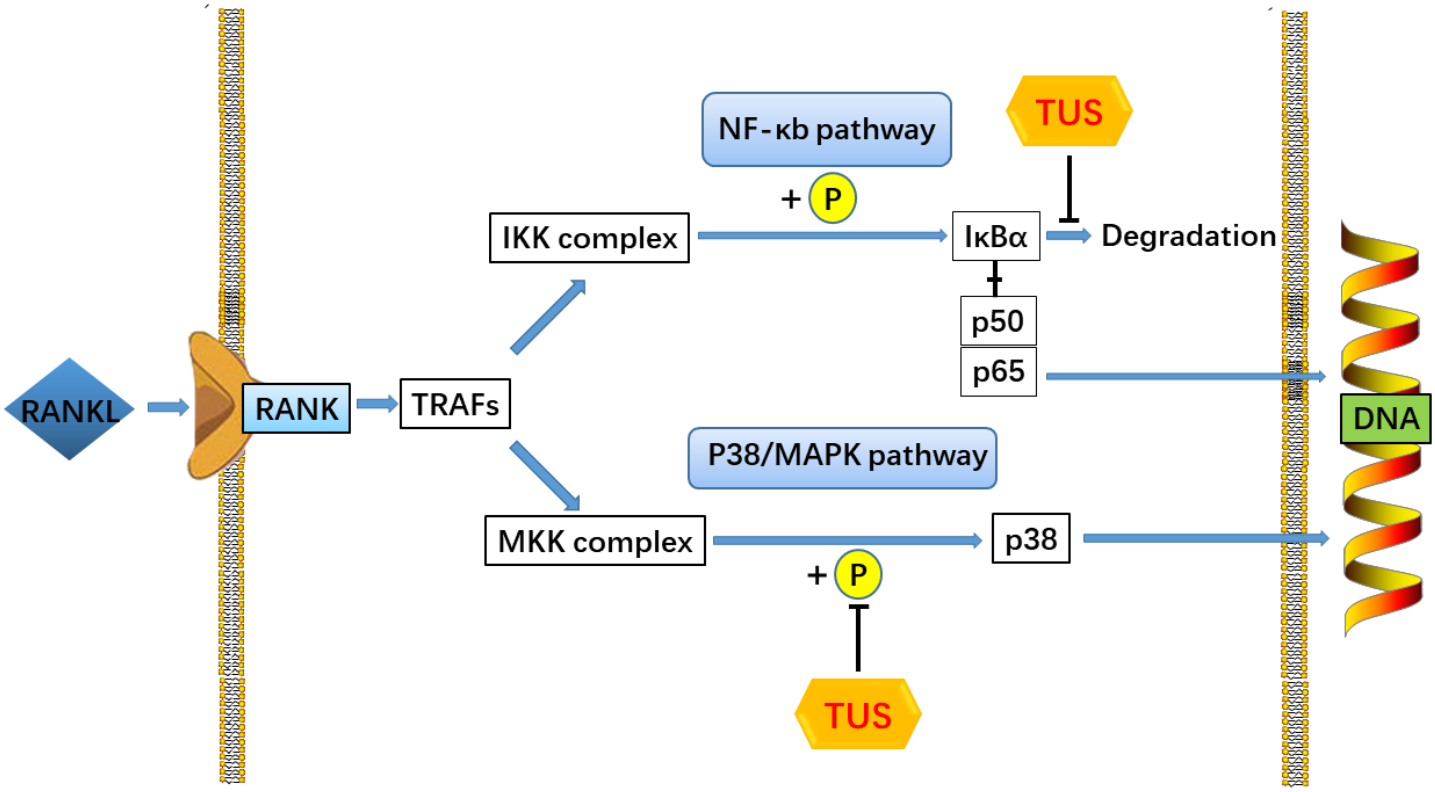

Figure 14

A pattern diagram of TUS in down-regulating osteoclastogenesis. By targeting the degradation degradation of IκBα and phosphorylation of p38, TUS suppressed RANKL-induced expression of osteoclast specific genes to inhibit osteoclast formation and functions in vivo and in vitro.